Journal of Organometallic Chemistry 787 (2015) 33–43

Contents lists available at ScienceDirect

Journal of Organometallic Chemistry

journal homepage: www.elsevier.com/locate/jorganchem

Quantum mechanical study of the kinetics, mechanisms and thermodynamics of the gas-phase decomposition of $Pb[(^{i}Pr)_2PSSe]_2$ single-source precursor

Francis Opoku, Noah Kyame Asare-Donkor*, Anthony Apeke Adimado

Department of Chemistry, Kwame Nkrumah University of Science and Technology, Kumasi, Ghana

ARTICLE INFO

Article history:
Received 19 January 2015
Received in revised form
23 March 2015
Accepted 14 April 2015
Available online 22 April 2015

Keywords:
Density functional theory
Gas phase
Decomposition
Reaction mechanism
Precursor

ABSTRACT

The reaction mechanism of the gas phase decomposition of $Pb[(^{i}Pr)_2PSSe]_2$ single-source precursor has been investigated theoretically by means of the density functional theory (DFT). The geometries of all the stationary points and the selected points along the potential energy surfaces were optimized at the M06/LACVP* level of theory. The harmonic vibrational frequencies of all the stationary points were calculated at the above same level of theory. Ten possible reaction pathways including seventeen reaction pathways on both the singlet and doublet potential energy profiles were explored. The results indicate that the steps that lead to PbS formation on both the singlet and the doublet potential energy surfaces are favored kinetically over those that lead to PbSe and ternary $PbSe_xS_{1-x}$ formation. However, thermodynamically, the steps that lead to ternary $PbSe_xS_{1-x}$ formation are more favorable than those that lead to PbSe and PbS formation on the doublet PESs. Moreover, the energetics also suggests the proposed scheme involving the dissociation of PbSe to be the most stable species on the singlet PES. Density functional theory calculations of the gas phase decomposition of the complex indicate that the deposition of ternary $PbSe_xS_{1-x}$ in chemical vapor deposition may involve more than one steps but the steps that lead to the its formation are consistent with a dominant role for thermodynamic factors, than kinetic.

Introduction

Metal-organic compounds have been used as single-source precursors to deposit a variety of thin-film materials at low temperature. Single-source precursor allows a good control of the gas phase composition up to the deposition zone and is useful for simplification of the reactor design and processing conditions. In chemical vapor deposition (CVD) applications, precursors of isopropyl derivatives are better than the phenyl-substituted derivatives in terms of volatility [1]. Thus, isopropyl derivative is of paramount interest as single-source precursors for the deposition of metal chalcogenide thin films [2,3].

The metal dithiophosphinates, $M[S_2PR_2]$, is an important class of organophosphorus compounds [4]. Less attention has been paid to the selenium analogs, the diselenophosphinates, $M[Se_2PR_2]$ [5], however, their chemistry is developing rapidly. The mixed metal thioselenophosphinates, $M[SeSPR_2]$, have been virtually been ignored, due to the lack of expedient methods for their synthesis, but are of special interest because the bridging S- and Se-donor atoms has a distinctive structural diversity as a results of their abilities to deposit metal chalcogenides of unpredictably useful proprieties. Metal thioselenophosphinates are useful starting materials for the preparation of both S and Se derivatives of thioselenophosphinic acids [6] as well as metal complexes [7], and useful as single-source precursors for the deposition of desired nanomaterials and thin films. Panneerselvam et al. has employed silver(I) thioselenophosphinate, $[Ag(SeSP^{i}Pr_2)]_4$, as single source precursor to deposit Ag_2Se thin films using aerosol-assisted and low-pressure chemical vapor deposition methods [8]. O'Brien et al. have also reported the use of lead(II) thioselenophosphinate, $Pb[SeSPPh_2]_2$, precursor for the deposition of PbSe micro- and nanocrystals [9]. Lead chalcogenides, PbE (E = S, Se, Te), as thin films have been of considerable interest [10]. One driving force is the recently discovered phenomenon of multiple exciton generation (MEG) [11], which could ultimately lead to more efficient solar energy conversion [12,13]. Lead sulfide nanoparticles may be useful in electroluminescent devices such as light-emitting diodes. In

---

* Corresponding author. Tel.: +233 205377408; fax: +233 3222060305.
E-mail addresses: ofrancis2010@yahoo.co.uk (F. Opoku), asaredonkor@yahoo.co.uk (N.K. Asare-Donkor), tonyadimado@yahoo.co.uk (A.A. Adimado).

http://dx.doi.org/10.1016/j.jorganchem.2015.04.013
0022-328X/© 2015 Elsevier B.V. All rights reserved.

addition, the exceptional third-order non-linear optical properties of PbS nanoparticles have potential applications in high-speed switching [14]. The structure of $Pb[(^{i}Pr)_2PSSe]_2$ complex are shown in Fig. 1.

Structural information such as geometrical and electronic configurations, molecular dynamics as well as thermodynamic and magnetic properties of the dichalcogenophosphinates complexes is important for understanding the different factors influencing their practically useful properties [15]. The structural investigations of metal phosphinates provide an insight into the decomposition processes occurring at the chemical vapor deposition of metal chalcogenides as well as can guidance on the design of more selective deposition process for CVD process of single-source precursors.

To the best of our knowledge, theoretical studies of decomposition of $Pb[(^{i}Pr)_2PSSe]_2$ precursor employing quantum chemical methods are yet to be reported. In addition experimental deposition of ternary $PbSe_xS_{1-x}$ alloys by the CVD method is limited, wherein x is the mole fraction of Se and $1-x$ is the mole fraction of S, with x gradually changing within a range wherein $x < 1$ and $x > 0$. In this study, decomposition pathways of Pb(II) square planar thioselenophosphinate, $Pb[(^{i}Pr)_2PSSe]_2$ complex were investigated in the gas phase to shed more light into the detailed mechanism of the chemical vapor deposition process involved in the deposition of single-source precursors. Several possible decomposition pathways were proposed, and the most favorable pathway were determined.

Computational methods

All calculations were carried out with Spartan 10 v1.1.0 Molecular Modeling programs [16] at the DFT M06/LACVP* level of theory. The LACVP* basis set is a relativistic effective core-potential, developed by Dunning, for first row elements [17] and the Alamos ECP plus double zeta basis set developed by Wadt and Hay for the atoms Na–La, Hf–Bi [18–20]. The LACVP* basis set is the most successful basis set in Spartan for the study of heavy transition metal chemistry and is the most commonly used basis sets. The M06 is a novel hybrid *meta* functional with good accuracy for applications involving main group thermochemistry, organometallic and inorganometallic thermochemistry, noncovalent interactions and kinetics [21–24].

The starting geometries of the molecular systems were constructed using Spartan's graphical model builder and minimized interactively using the sybyl force field [25]. All geometries were fully optimized without any symmetry constraints. A normal mode of analysis was performed to verify the nature of the stationary point and equilibrium geometries were characterized by the absence of imaginary frequencies.

The transition state structures were located by series of constrained geometry optimization in which the breaking bonds were fixed at various lengths and optimized the remaining internal coordinates. The approximate stationary points located from such a procedure were then fully optimized using the standard transition state optimization procedure in Spartan. All first-order saddle points were shown to have a Hessian matrix with a single negative eigenvalue, characterized by an imaginary vibrational frequency along the reaction coordinate. All the computations were performed on Dell Precision T3400 Workstation computers. ChemDraw Ultra 12.0 graphical software was used to draw the energy profile and the Mercury 3.3 software was used to visualize the optimized structures.

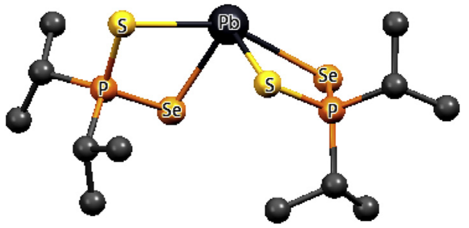

Fig. 1. Structure of the optimized $Pb[(^{i}Pr)_2PSSe]_2$ precursor.

The rate constants were calculated using the transition state theory for all elementary steps involved in the gas phase decomposition. The unimolecular rate constant, k_{uni} and equilibrium constants, Keq were computed using Equations (1) and (2) respectively, which were derived from the transition state theory [26,27] and assuming that the transmission coefficient, κ is equal to 1.

$$k_{uni} = \left(\frac{\kappa k_B T}{h}\right) \exp^{-\left(\frac{\Delta G^{\ddagger}}{RT}\right)} \tag{1}$$

$$K_{eq} = \exp(-\Delta G^{o}/RT) \tag{2}$$

The recombination rate constants (k_{rec}) from the kinetics is

$$k_{rec} = K_{eq} \times k_{uni} \tag{3}$$

where $\Delta G^{\ddagger}$ is the activation free-energy, ΔG^{o} is the Gibbs free energy, and k_B and h are the Boltzmann and Planck constants, respectively.

Mechanistic considerations

The reaction pathways for the gas phase decomposition of $Pb[(^{i}Pr)_2PSSe]_2$ complex were based on the schemes suggested by Akhtar et al. [9] and Opoku et al. [28–30]. The species considered are (i) the dissociation of PbSe, (ii) the dissociation of PbS, and (iii) the heterogeneous P–S and P–Se bond cleavages to form a ternary $PbSe_xS_{1-x}$. These have been presented in Schemes 1–4. The activation and reaction free energies were computed at $T = 800$ K.

Results and discussion

Optimized geometry of $Pb[(^{i}Pr)_2PSSe]_2$ precursor

The bond lengths and angles for the X-ray [9] and optimized geometries of the $Pb[(^{i}Pr)_2PSSe]_2$ complex are shown in Table 1. The lead centre has a distorted square pyramidal geometry with the ligand bond angles of 75.99° and 76.28° which are smaller than the perfect square planar angle, but the angles are slightly wider than those in the $Pb[(C_6H_5)_2PSSe]_2$ precursor analog [29]. The density functional theory (DFT) geometry optimization on a potential energy surface (PES) has the Pb–S bond length at 2.83 Å, as expected, shorter than the bond length of Pb–Se (2.90 Å). The significant disparity in the Pb–Se bond distance at 3.01 A° suggests a stereochemical influence from the lone pair on the metal centre. The distortions from the ideal geometry as evident in the wider S–Pb–Se bond angle of 153.81° was as a result of the proximity of the non-coordinating S- and Se-donor atoms to the Pb(II) atom.

Overall decomposition of $Pb[(^{i}Pr)_2PSSe]_2$ precursor

The reaction mechanisms for the gas phase decomposition of $Pb[(^{i}Pr)_2PSSe]_2$ precursor were studied at the M06/LACVP* level of theory by considering the energetics of the reactants, transition states, intermediates, and products of the given reactions. In order